

Eleven microphones were used that were more closely spaced (10° to 15° intervals) near the nozzle jet than in the upstream quadrant (15° to 20° intervals). The angle $\theta_I = 0^\circ$ is directed upstream. This vertical circular array of half-inch condenser microphones (with windscreens) was located above 6-inch thick acoustic foam on the ground. This microphone and foam arrangement resulted in free field noise data in the far field for frequencies above 400 Hz. The microphones were calibrated before and after each day's run with a piston calibrator (a 124 dB tone at 250 Hz).

The noise data were analyzed directly by an automated one-third octave band spectrum analyzer, which was periodically recalibrated, and also checked with a pink noise generator. The analyzer determined sound pressure level spectra, SPL, referenced to 0.0002 microbar (2×10^{-5} N/m²). A small fraction of the data required corrections. Background noise affected the low noise level data below 400 Hz; the data were corrected to remove this contribution. Generally three samples of data were taken so that occasional transient background noises could be eliminated by a voting and averaging scheme in the data processing program. A small correction (about 2 dB at 20 kHz) was also made, according to SAE ARP866,⁽⁴⁾ for atmospheric losses so that the data reported are lossless. These SPL spectra were then used to compute the overall sound pressure level, OASPL, at each microphone position. Occasionally the peak SPL occurred too close to the highest frequency recorded (20 kHz), causing the computed OASPL to be too low. These SPL spectra were extrapolated and the OASPL was thereby corrected (less than 2 dB). Lip noise, which is a non-jet noise (generally affecting a few 1/3 octave bands near or above 20 kHz), was also not included in the OASPL. The sound power level spectrum, PWL, and total sound power level, PWL_T, were computed by a spatial integration of the SPL spectra. The spatial integration used the "bread slice" elements for this axisymmetric noise, as described in Ref. 5.

From the microphone calibrations, periodic checks of the data system, and redundant data it was estimated that the data were repeatable from day to day to about 1 dB and a third octave band. Most of the directly compared data were taken on the same day, and these data were repeatable to about 1/2 dB. In Ref. 6, some of the single stream jet noise spectral data obtained from this facility were compared to scaled up data taken by Lush in an anechoic chamber⁽⁷⁾; the agreement was within the day to day repeatability.

The data reported herein are considered to be accurate, lossless, far and free field pure jet noise.

Test Nozzles

Figure 2 contains sketches of the two-stream coaxial nozzles tested and part of the nozzle inlet geometry. Because the nozzle flange was far enough upstream and the nozzle inlets were not excessively large, there was no significant jet noise reflection or shielding affecting the noise radiation pattern at angles greater than 30° . Figure 2(a) schematically shows the coplanar nozzle configuration that was used for most of the



description of its noise level and its spectra. The noise level for ambient temperature subsonic single stream nozzles was described in Ref. 6. However, jet noise spectra have not been adequately described. A correlation of jet noise spectral data is required.

The ambient temperature subsonic jet noise spectral data are described herein by a series of spectral templates, one for each angle, whose shape is essentially unaffected by nozzle size and only slightly affected by the jet velocity. The location of the peak noise on each template is defined by its level, SPL_p , and frequency, f_p . For an ambient temperature jet, the location of the peak noise (SPL_p , f_p) is a function of jet velocity, nozzle size, and angle. The peak noise level, SPL_p , is determined by two relationships. One empirically relates the difference, $OASPL - SPL_p$, to the angle. The other relationship is for the total intensity, $OASPL$, which was defined in Ref. 6 as a function of nozzle size, jet velocity, and angle. Once the peak noise is located in noise level and frequency space (SPL_p , f_p), then the spectral template for that angle defines the rest of the noise spectrum.

Figure 3 shows the spectral shape curves (templates) for jet noise at a number of angles, for $\frac{1}{8}$ -, 4-, and 6-inch diameter nozzles at high and low subsonic velocities.^(6,8) The spectral data are plotted in a manner that describes the jet noise spectra relative to the peak noise (SPL_p , f_p), which is determined as described above. A gradual change in the spectral shape occurs with angle. The change in shape is rapid near the jet axis, where refraction is important. The spectral shape is also broader near the jet axis at the low jet velocities than for the high velocities. The template curves were constructed as follows. Each spectral data set for a given nozzle velocity and angle, was translated (without rotation) as a unit in order to get the best agreement between the data sets at each angle. This translation was required for two reasons. One is caused by the variation of f_p with velocity and size. The other is due to the fact that the spectral shape was observed to translate by as a whole by as much as 1 dB and a third octave band in long term repeatability experiments. After the data sets are collapsed together one average smooth curve was drawn through the data points for each angle and velocity as shown on Fig. 3. The difference between the total intensity and peak noise level ($OASPL - SPL_p$) is calculated from these curves and noted on Fig. 3; this difference is used later.

These spectral templates were then used to locate the peak noise frequency, f_p , of other single stream nozzle jet noise data, which covered a subsonic velocity range of 600 to 1000 ft/sec and a nozzle diameter range of from 1 to 6 inches.^(6,8) The location of the peak noise (SPL_p , f_p) can be quite accurately determined because the applicable template is translated until the best overall fit is obtained for the 20 to 25 data points of a spectral set. The resulting experimental values of f_p , referenced to the f_p at $\theta_I = 90^\circ$, are plotted on Fig. 4 as a function of angle, θ_I . These data show that there is no f_p variation with angle in the upstream quadrant ($\theta_I < 90^\circ$), but for $\theta_I > 90^\circ$ there is a rapid change in f_p with angle. There appears to be a small effect of



velocity but only near the jet axis.

All that remains to be done is to relate f_p at $\theta_I = 90^\circ$ to the jet velocity, V_C , and the nozzle size, d_C . This was accomplished by using the following equation

$$f_p(\theta_I = 90^\circ) = 1.0 \frac{V_C}{d_C} \quad (1)$$

With the baseline single stream (or core jet alone) noise correlated the next task is to consider the modifications of the core noise caused by the fan flow.

Coplanar Coaxial Nozzle Jet Noise Data

In this section the modification of the single jet noise caused by the addition of the fan flow to the core flow is considered. It will be shown that the noise level of a coaxial nozzle is essentially a modification of the core-nozzle-alone peak noise level and frequency. The spectral template that described the core-alone jet noise spectra is unchanged by the fan flow. The template just translates as a function of the coaxial nozzle parameters.

Noise Level. The influence of the fan flow upon the noise level and noise radiation pattern shape is considered in this section. The data taken in this study and in Ref. 1 both show that the shape of the noise radiation pattern is independent of the fan flow. In other words the pattern shape is unaffected by changes in the coaxial nozzle parameters (i.e., the fan to core area ratio, $AR = A_F/A_C$, and velocity ratio, $VR = V_F/V_C$). The pattern shape is the same as for the core nozzle alone. Only the noise level changes as a function of the coaxial nozzle parameters, VR and AR . Based on these results the following equation was written to describe the noise level and radiation pattern for the coaxial nozzle.

$$\text{OASPL} = 10 \log_{10} \left[\underbrace{\frac{K}{R^2} \frac{\rho_o^2}{c_o^4} A_C V_C^8}_{\text{Core jet alone noise level}} \underbrace{\left(1 - \frac{0.62 V_C}{c_o} \cos \theta_J \right)^{-3}}_{\text{Shape of noise radiation pattern}} \underbrace{\Gamma(AR, VR)}_{\text{Effect of fan flow}} \right] + C \quad (2)$$

The coefficient, K , which is determined from single stream jet noise data at $\theta_J = 90^\circ$, is equal to 3.2×10^{-6} . The core-jet-alone noise level is described by the first group of terms while the effect of the fan flow on the noise level is described by Γ , which is a function of only the coaxial nozzle parameters, VR and AR . The noise radiation pattern shape



from the change in OASPL at 90° . The same result was also obtained using the change in total sound power. The change in sound power data reported in Ref. 2 and the change in OASPL at 120° , measured by Williams,⁽¹⁾ are also plotted on Fig. 9. The results from the literature closely agree with the results obtained in this study.

Results from the SAE model are plotted on this figure as dashed curves. The SAE coaxial jet noise prediction⁽¹¹⁾ assumes each jet (the fan and core) generates noise independently. This means the noise cannot be less than the core alone, which is obviously erroneous for $VR \leq 0.6$, based on Fig. 9. However, this prediction is accurate for $VR \geq 0.8$, which is where most present day turbofan engines operate.

To summarize, the peak noise level, SPL_p , is determined from Eq. (3) for $\Gamma\langle AR, VR \rangle$, Eq. (2) for the OASPL, and Fig. 3 for $(OASPL - SPL_p)$.

Spectra. When the peak noise level, SPL_p , has been determined all that remains to be done in order to completely define coplanar coaxial jet noise is to determine the frequency of the peak noise, f_p , as a function of VR and AR. With SPL_p and f_p determined, the spectral templates can then be positioned to describe the whole of the coaxial jet noise spectral surface, $SPL\langle f, \theta_I \rangle$. From the peak noise locus curves of Fig. 7, and other similar data, the variation in f_p with VR and AR can be determined. Figure 10 contains a plot of the peak noise frequency ratio as a function of VR and AR. The peak noise frequency ratio, $F_{pR}\langle AR, VR \rangle$, is defined as the f_p , measured at VR and AR, divided by the f_p of the core jet alone (at $VR = 0$). The f_p for the core alone is determined from Eq. (1) and Fig. 4. Average smooth curves are drawn through the data for each velocity ratio, VR. The $VR = 0.4$ curve is not drawn for $AR > 16$ because of the two-peaked spectra that develop at $VR = 0.4$ somewhere between an AR of 16.4 and 27. The data scatter generally within a one-third octave wide band from these curves. While the data shown are for $\theta_I = 90^\circ$ and a core velocity of about 985 ft/sec, the same overall results are obtained at other angles and core velocities.

To summarize, the peak noise frequency, f_p , of a coaxial nozzle is determined by the following relationship.

$$f_p = \underbrace{F_{pr}\langle \theta_I \rangle}_{\text{Core jet alone}} \left(\frac{1.0 V_C}{d_C} \right) \underbrace{F_{pR}\langle AR, VR \rangle}_{\text{Effect of fan flow}} \quad (4)$$

where $F_{pr}\langle \theta_I \rangle$ is determined from Fig. 4 and $F_{pR}\langle VR, AR \rangle$ is determined from Fig. 10.

At $VR = 1$ the coaxial nozzle might be expected to act as a single nozzle whose diameter is that of the fan nozzle. This would mean that at



tion noise. The blunt ended plug is an extreme academic example of flow separation, but the results point out the importance of avoiding flow separation in a suppressor nozzle, such as the coaxial nozzle, operating at conditions near maximum suppression (e.g., $VR = 0.5$).

Extended Core Nozzle. The velocity in the fan exhaust will decay as it flows downstream. If the core nozzle is extended a considerable distance downstream of the fan nozzle, then a jet velocity ratio of unity might become a local velocity ratio of about 0.5 at the core exit plane. A greatly extended core nozzle might therefore have its minimum coaxial jet noise occurring at $VR = 1$. The core extension test nozzles had an area contraction at the exit as shown by Fig. 2(c). This resulted in a low turbulence uniform velocity profile at the core exit. The noise from a long core nozzle extension (56 annulus heights long) was compared to a short core nozzle extension (8.5 annulus heights long). The outer nozzle size would have to be changed in order to directly compare to a coplanar nozzle, but Fig. 11(a) shows that the short core nozzle extension coaxial nozzle produced the same noise as an equivalent size coplanar circular coaxial nozzle. Therefore the long extension is effectively compared to a coplanar nozzle. Figure 12 contains a comparison of the power spectra for the long and short core nozzle extensions for three velocity ratios ($VR = 0, 0.5, 1.0$). The spectra are the same for $VR = 0$ and 0.5. But when $VR = 1$ the long core extension is somewhat quieter at low frequencies. The velocity profile was measured at the core exit plane for the short core extension. The fan nozzle exhaust velocity profile there is rounded but the peak velocity is the same as the fan jet velocity (i.e., $V_E/V_F = 1$). In the case of the long core extension, the fan exhaust (peak velocity) decayed to half of fan jet velocity, $V_E/V_F = 0.5$, by the time it reached the core exit plane.

In conclusion, a small noise reduction can be achieved at $VR = 1$ by a core nozzle extension, but only if it is extremely long.

Extended fan nozzle. In many engine designs the fan nozzle is extended beyond the core nozzle exit plane. This permits some mixing of the hot core and cold fan flows, which can theoretically increase the thrust. The extended fan nozzle geometry tested herein is shown in Fig. 2(d). In this case the fan nozzle extension was a constant diameter pipe. The fan extensions tested ranged from 2 to 6 fan nozzle diameters long (e.g., $L_F/d_F = 2, 4, 6$). Complete internal mixing occurred (i.e., the velocity profile is essentially unaffected by additional length) for the 6 diameter long case⁽¹⁾ and partial mixing occurred with the shorter lengths.

The extended fan nozzle cases are compared to the coplanar nozzle case ($L_F/d_F = 0$) at the same core nozzle exit plane velocities (V_F, V_C). Figure 13(a) shows the change in noise as the velocity ratio ($VR = V_C/V_F$) was varied for each of the extension cases ($L_F/d_F = 2, 4, 6$). The change in noise is the change from the coplanar nozzle case at $VR = 0$ (for coplanar nozzles $VR = 0$ is acoustically equivalent to running without the fan nozzle, $AR = 0$). This comparison is for an area ratio of 3.9, a core

velocity of 740 ft/sec and a core nozzle diameter of 3 inches. The data show that there is a small decrease (less than 2 dB) in the noise level for velocity ratios greater than 0.8 when the fan nozzle is extended. The spectral data (Fig. 13(b)) and noise radiation pattern are also essentially unchanged. Williams⁽¹⁾ noted essentially the same result in a similar experiment with smaller nozzles. At the low velocity ratios there was a general increase in the noise level at all frequencies (see Fig. 13(a) and (b)). For the $L_F/d_F = 2$ and 4 cases there was an additional intense low frequency broadband howling noise. The noise radiation pattern for these low velocity ratio cases peaked at about $\theta_I = 130^\circ$ while the coplanar and high velocity cases peaked near 160° . The former result is characteristic of an internal noise source, while the latter is characteristic of an external noise source. The table contained in Fig. 13(a) indicates the extended fan nozzle exhaust plane peak (centerline) velocity, V_E , for each case, compared to the core velocity ($V_C = 740$ ft/sec). For the large velocity ratio cases there was very little decay of the centerline velocity (i.e., $V_E/V_C \approx 1$). This fact coupled with the fact that the noise radiation pattern is characteristic of an external noise source, indicate that the major part of the jet noise is generated by the external exhaust jet for the high velocity ratio cases. At low velocity ratios most of the noise is being generated within the extended fan nozzle.

Similar tests were performed with a nozzle of small contraction (upstream area/nozzle exit area = 1.2) attached to the extended fan nozzle exit. The core nozzle exit plane velocities (V_C, V_F) were the same as for the no exit nozzle cases described above. This exit nozzle caused V_E/V_C to exceed 1 except at very low velocity ratios. Therefore the external jet was even more clearly the dominant noise source except at very low VR, where there was still an intense howling noise.

These extended fan nozzle results point out that the majority of the jet noise occurs wherever the velocity decay is largest. In these ambient temperature experiments, the peak (centerline) velocity did not decay much internally at the high velocity ratios; therefore, the external jet was the dominant jet noise source. If the core jet were hot there may be more internal decay; therefore, the results may be different.

Three-stream nozzle. If each stage of a two-fan stage turbofan engine were exhausted separately, then the resulting engine would have three exhaust streams. One such arrangement was tested and the results are shown in Fig. 14. In this configuration the fan (middle nozzle) to core area ratio was 2.1, the outer nozzle to fan nozzle area ratio was 0.78, and the core diameter was 3 inches. The outer nozzle to fan nozzle velocity ratio, V_O/V_F , varied from 0.8 to 0.7 as the fan to core velocity, $VR = V_F/V_C$, was changed from 1.0 to 0.5. For comparison, the outer nozzle was blocked and the resulting two stream nozzle was run at the same velocity ratios, VR. Even though the total flow for the three stream nozzle was much larger it was slightly quieter than the two stream nozzle at the same VR and core conditions.



Noise Radiation Pattern of Internal Noise

This section discusses tests performed in order to describe the noise radiation pattern of engine fan and turbine noise passing through a coaxial nozzle. These noise sources were simulated by a dominant internal noise placed upstream of each nozzle.

A dominant internal noise of high frequency was first placed in the core nozzle plenum and the fan flow was varied from $VR = 0$ to 1, for a fixed core velocity. The internal noise was generated by a half-inch orifice that exhausted far upstream into the core nozzle plenum. At a frequency of 10 kHz the internal noise was at least 6 dB more than the jet noise at all angles, for velocity ratios between 0 and 1. The pressure ratio across the noise orifice was held constant so that the internal noise level would be nearly constant. The sound power level, PWL, at 10 kHz did in fact remain constant with the internal noise in the core. Figure 15(a) shows how this constant power internal core noise distributes spatially (i.e., noise radiation pattern) at a frequency of 10 kHz for velocity ratios of 0, 0.5, and 1 at core velocities of 600 and 860 ft/sec. The noise radiation pattern for internal core noise passing through a nozzle appears to peak near $\theta_I = 110^\circ$, and is fairly independent of the fan or core flow. Refraction caused by the fan flow reduced the noise near the jet axis only about 4 dB.

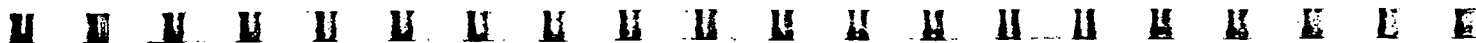
The same experiment was repeated with the internal noise placed instead in the fan nozzle plenum. In this case the PWL at 10 kHz varied some with VR, so the noise levels had to be adjusted. Figure 15(b) shows that almost the same radiation pattern as Fig. 15(a) resulted, but with the peak noise moved downstream to 120° . In these experiments the wave length of the internal noise is much less than the nozzle diameter; this is also the case for turbofan engines. The ambient temperature results in Figs. 15(a) and (b) are typical of engine turbine and fan noise radiation patterns in that they also peak near 120° .⁽¹²⁾ These data should prove useful in evaluating engine noise data, which is a complex mixture of noise sources.

Summary of Results

Free field pure jet noise data were taken for a large range of coaxial nozzle configurations. The core nozzles were circular (1 to 4 in. diam.) and plug types. The fan-to-core area ratio varied from 0.7 to 43.5, while the velocity ratio typically varied from 0 to 1. For most cases the two nozzles were coplanar, but large axial extensions of either nozzle were also tested. The data and correlations are limited to ambient temperature jets.

The important results and correlations are described below.

1. The fan flow from a coaxial nozzle essentially modifies the core nozzle alone jet noise. The noise level, OASPL, for the coaxial nozzle is equal to the multiple of two terms. The first term describes the core



nozzle alone noise level and radiation pattern. The second term, Γ , which is the only term dependent on the fan flow, affects only the noise level. The minimum noise level for a given nozzle and core velocity occurs at a fan to core velocity ratio of 0.4 to 0.5. The coaxial nozzle noise level data are well correlated by the semiempirical relations presented herein. These data agree well with the previous coaxial jet noise data reported by T. Williams and G. Bielak.

2. The SPL spectral shape at a given angle did not significantly change with core nozzle size, or with the velocity and area ratios. In other words, if the location of the peak noise (both level, SPL_p , and frequency, f_p) is known, then the spectral shape (template) for that angle could be used to construct the complete spectrum. These spectral templates are given in the text. The peak noise level, SPL_p , is determined from the OASPL. The peak noise frequency, f_p , for a coaxial nozzle is equal to the multiple of three terms. The first two terms describe the peak noise frequency for the core jet noise alone. The last term is the ratio of the coaxial noise to the core alone noise, and is only a function of the velocity and area ratios. The minimum f_p occurs at a velocity ratio of 0.5 to 0.6.

3. The preceding results are for coplanar circular coaxial nozzles; the following results are for different nozzle geometries.

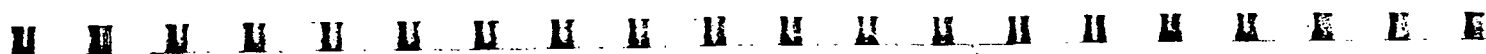
(a) The only significant difference between plug and circular coaxial nozzles of the same area is that the noise level of the plug nozzle is 1 to 2 dB quieter. Any flow separation off the plug can generate considerable noise except at the high velocity ratios.

(b) Extending the core nozzle well beyond the fan nozzle had only a small effect on the noise, compared to the coplanar nozzles result.

(c) Fan nozzle extension configurations are slightly quieter than the coplanar configuration at high velocity ratios, but an intense low frequency broadband howling noise is generated within this fan nozzle extension at the low velocity ratios.

Nomenclature

A_C	core nozzle area at exhaust plane, ft^2
A_F	fan nozzle area at exhaust plane, ft^2
A_O	third (outer) nozzle area, ft^2
AR	fan to core area ratio, A_F/A_C
C	constant to account for reference conditions and unit conversion factors



c_o	speed of sound in environment, ft/sec
d_C	core nozzle diameter, ft
d_F	fan nozzle diameter, ft
$F_{PR} \langle VR, AR \rangle$	peak noise frequency ratio of coaxial nozzle; f_p for coaxial nozzle at VR and AR, divided by f_p for core alone ($V_R = 0$)
$F_{PR} \langle \theta_I \rangle$	peak noise frequency ratio of the core; f_p at θ_I divided by f_p at $\theta_I = 90^\circ$
f	third octave band center frequency, Hz
f_p	frequency of the peak noise intensity, Hz
$f_p \langle \theta_I = 90^\circ \rangle$	peak noise frequency for core alone (single jet) at $\theta_I = 90^\circ$
h	annulus height, ft
K	constant defined by Eq. (2)
L_C	length of core nozzle extension beyond fan nozzle exit plane, ft
L_F	length of fan nozzle extension beyond core nozzle exit plane, ft
OASPL	overall sound pressure level, dB
PWL	sound power level, dB
PWL_T	total sound power level, dB
R	distance from noise source (in experiments, the fan nozzle exit) to observer or microphone, ft
SPL	sound pressure level, dB
SPL_p	peak intensity or sound pressure level, dB
T_o	environment temperature, $^\circ F$
t	core nozzle lip thickness, ft
V_C	core jet velocity at nozzle exit plane (measured or calculated) based on one-dimensional isentropic theory, ft/sec

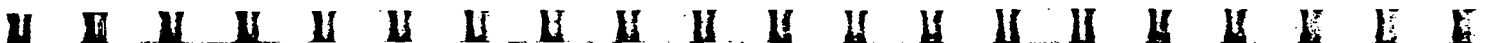
V_E	maximum velocity of decaying flow at extended nozzle exit plane, ft/sec
V_F	fan jet velocity, ft/sec
V_O	third (outer) nozzle jet velocity, ft/sec
VR	fan to core velocity ratio, V_F/V_C
$F(VR, AR)$	function relating coaxial nozzle noise level relative to that of the core, defined by Eq. (3)
θ_I	angle from nozzle inlet, deg
θ_J	angle from nozzle jet, $\theta_J = 180 - \theta_I$, deg
ρ_o	density of environment, lb_m/ft^3

References

1. Williams, T. J., Ali, M. R. M., and Anderson, J. S., "Noise and Flow Characteristics of Coaxial Jets," Journal of Mechanical Engineering Science, Vol. 11, No. 2, Apr. 1969, pp. 133-142.
2. Bielak, G. W., "Coaxial Flow Jet Noise," D6E-10041-1, 1972, Boeing/Aeritalia Co., Seattle, Wash.
3. Eldred, K., "Far Field Noise Generation by Coaxial Flow Jet Exhausts. Vol. I: Detailed Discussion," FAA-RD-71-101-Vol. 1, 1971, Wyle Laboratories, Inc., El Segundo, Calif.
4. Anon., "Standard Values of Atmospheric Absorption as a Function of Temperature and Humidity for Use in Evaluating Aircraft Flyover Noise," Aerospace Recommended Practice 866, Aug. 31, 1964, SAE.
5. Olsen, W. A., Miles, J. H., and Dorsch, R. G., "Noise Generated by Impingement of a Jet Upon a Large Flat Board," TN D-7075, 1972, NASA.
6. Olsen, W. A., Gutierrez, O. A., and Dorsch, R. G., "The Effect of Nozzle Inlet Shape, Lip Thickness, and Exit Shape and Size on Subsonic Jet Noise," AIAA Paper 73-187, Washington, D.C., 1973.
7. Lush, P. A., "Measurements of Subsonic Jet Noise and Comparison with Theory," Journal of Fluid Mechanics, Vol. 46, Pt. 3, Apr. 1971, pp. 477-500.
8. Karchmer, A., Dorsch, R., and Friedman, R., "Acoustic Tests of 15.2-Centimeters Diameter Potential Flow Nozzle," TM X-2980, 1974, NASA.



9. Goldstein, M. E., and Howes, W. L., "New Aspects of Subsonic Aerodynamic Noise Theory," TN D-7158, 1973, NASA.
10. Goldstein, M., and Rosenbaum, B., "Effect of Anisotropic Turbulence on Aerodynamic Noise," Journal of the Acoustical Society of America, Vol. 54, No. 3, Sept. 1973, pp. 630-645.
11. Anon., "Jet Noise Prediction," Aerospace Information Rept. 876, SAE, July 1965.
12. Staff, "Aircraft Engine Noise Reduction," NASA SP-311, 1972, pp. 32-33, 58-59, 186, 187, 190, 202, 204, 206, 211-213.



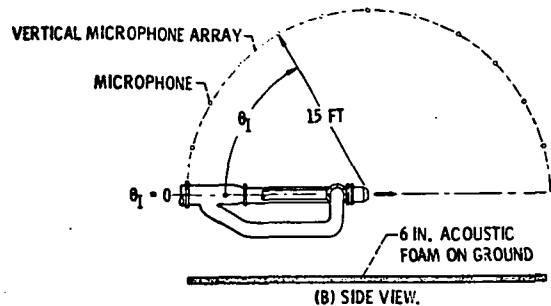
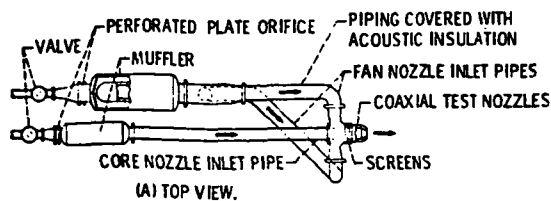


Figure 1 - Flow system for coaxial nozzle tests.

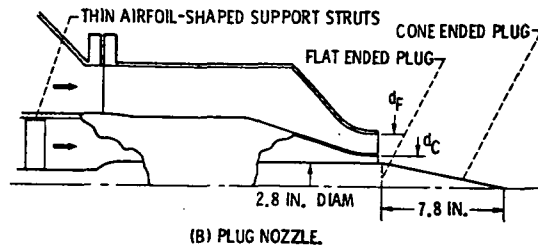
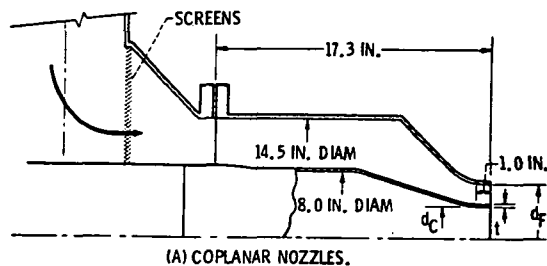


Figure 2 - Sketches of coaxial nozzles tested.

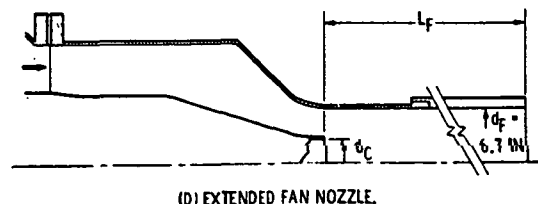
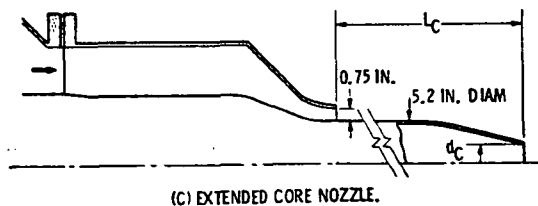


Figure 2 - Concluded.



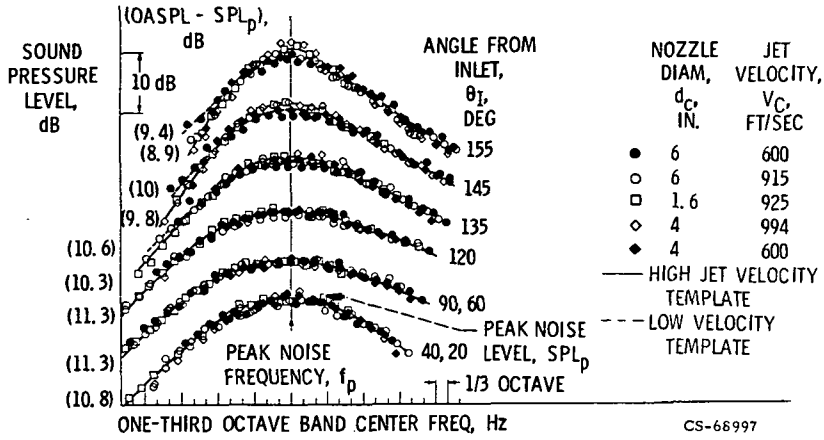


Figure 3. - Single stream (core) jet noise spectra shapes (templates). Ambient temperature subsonic circular jet; free field lossless data.

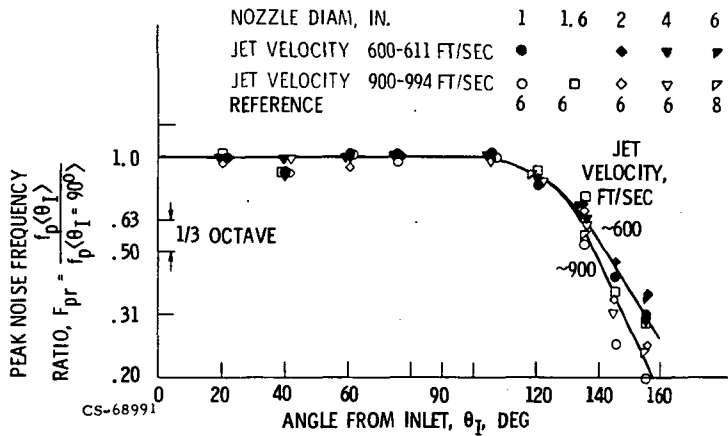


Figure 4. - Variation of the peak noise frequency with angle. Ambient temperature subsonic circular nozzles; free field lossless data.



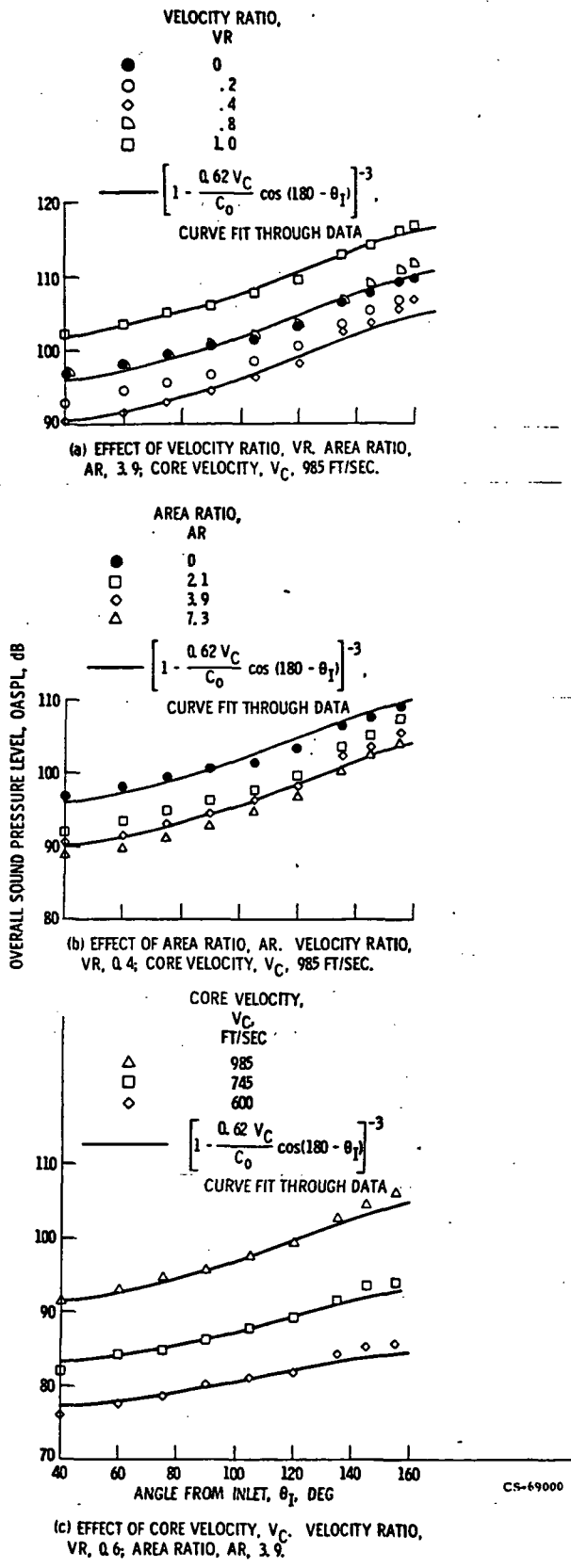
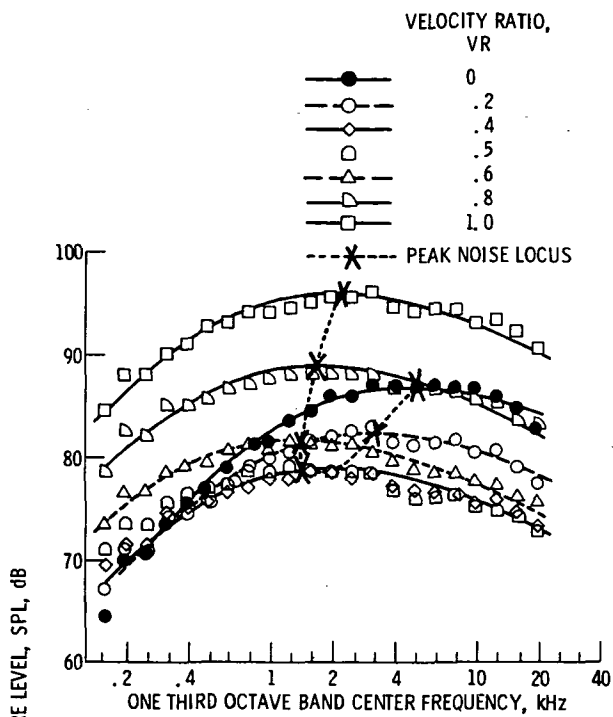
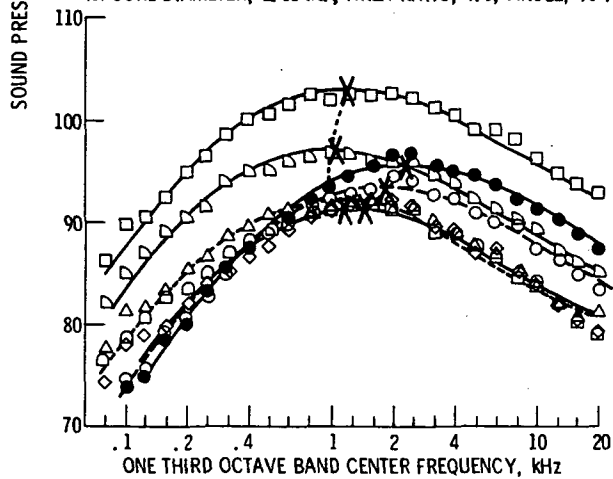


Figure 5. - Noise radiation pattern for coaxial nozzles at 15 feet. Core diameter, 3 in.; environmental temperature, 77° F; free field lossless data.



(c) CORE DIAMETER, 2.08 IN.; AREA RATIO, 9.3; ANGLE, 90°.



(d) CORE DIAMETER, 3 IN.; AREA RATIO, 3.9; ANGLE, 135°.

Figure 6. - Concluded.



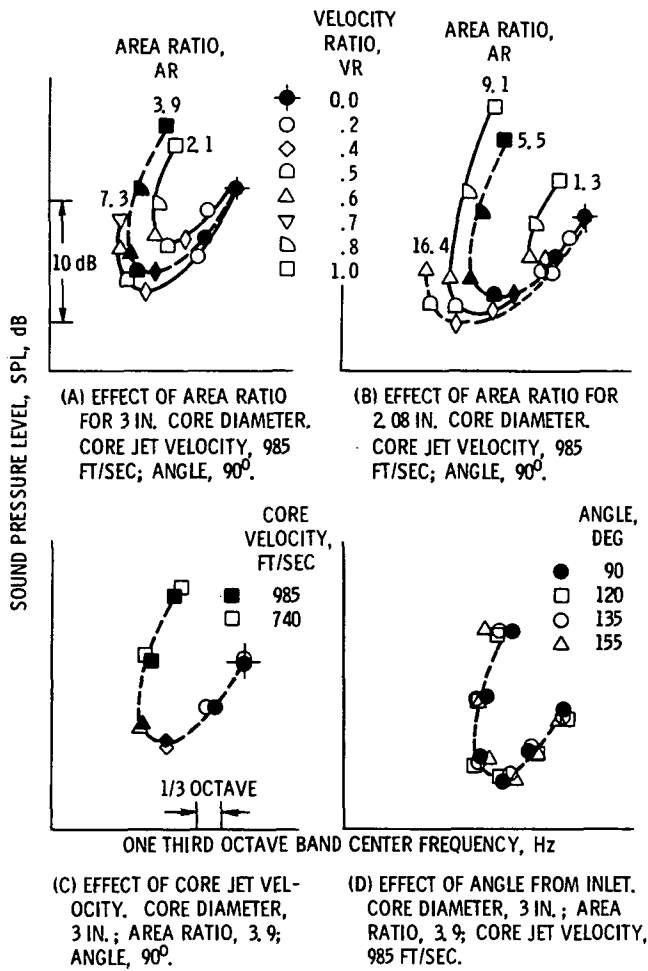
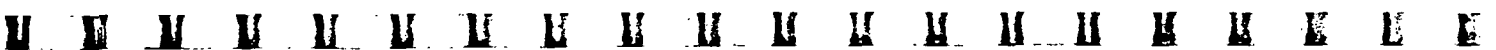


Figure 7. - Peak noise locus curve shapes for several coaxial nozzles. Circular coplanar nozzles; environmental temperature, 77° F; free field lossless data taken on a 15 foot radius.



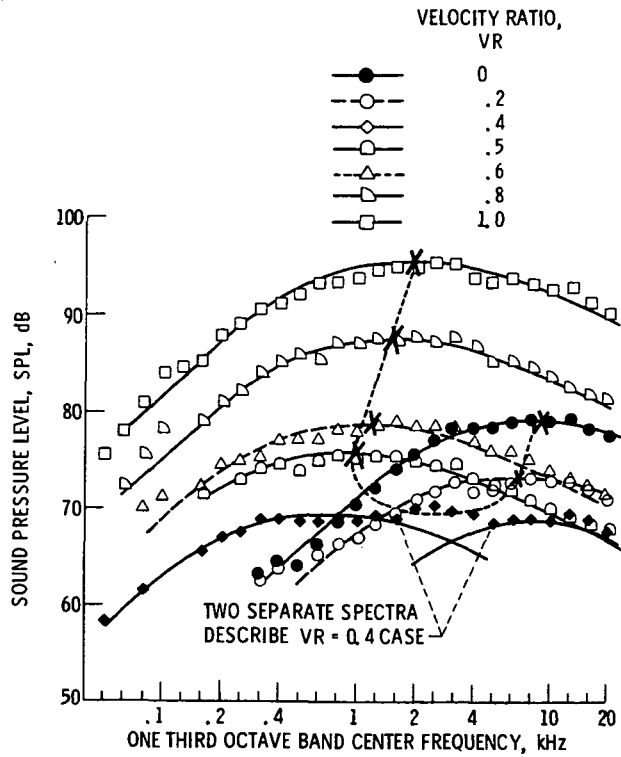


Figure 8 - Effect of velocity ratio on coaxial jet noise spectra at $\theta_T = 90^\circ$. Coplanar circular nozzles; area ratio, 43.5; core diameter, 1.0 inch; core jet velocity, 985 ft/sec; environmental temperature, 77° F; free field lossless data taken on a radius of 15 feet.

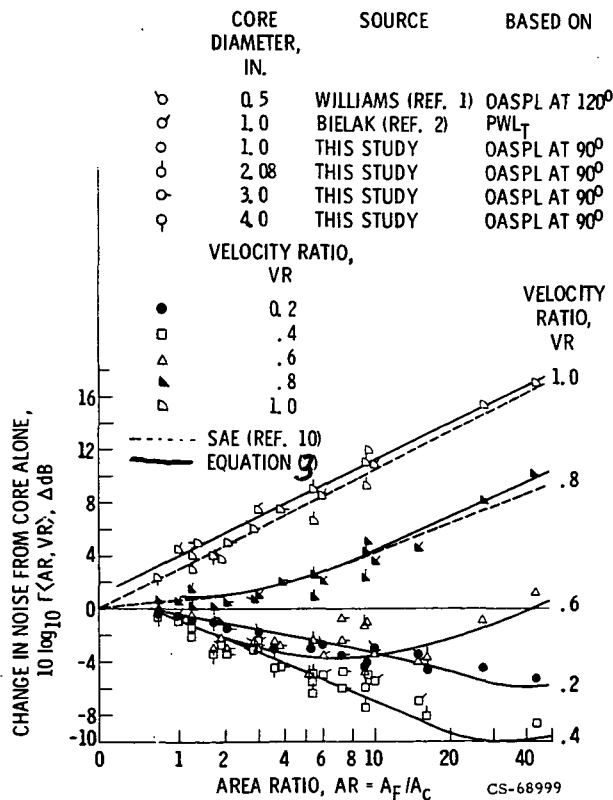
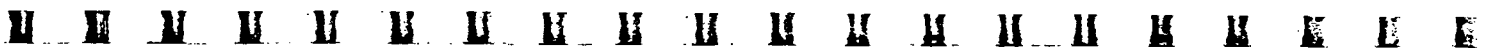


Figure 9. - Change in coaxial noise level, relative to the core alone noise level, with changes in area and velocity ratio.



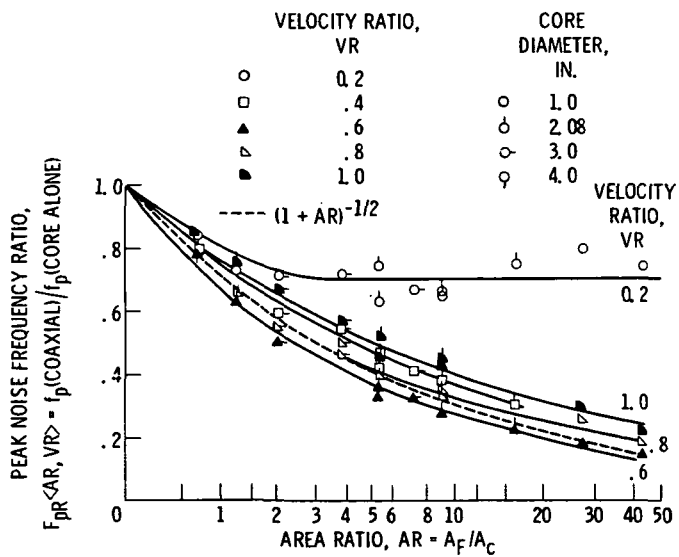
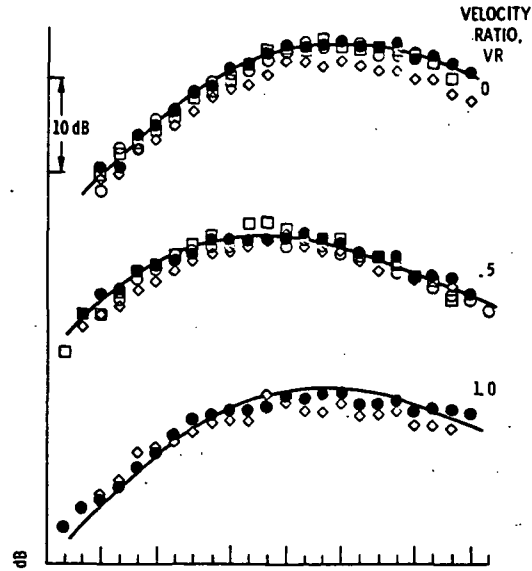


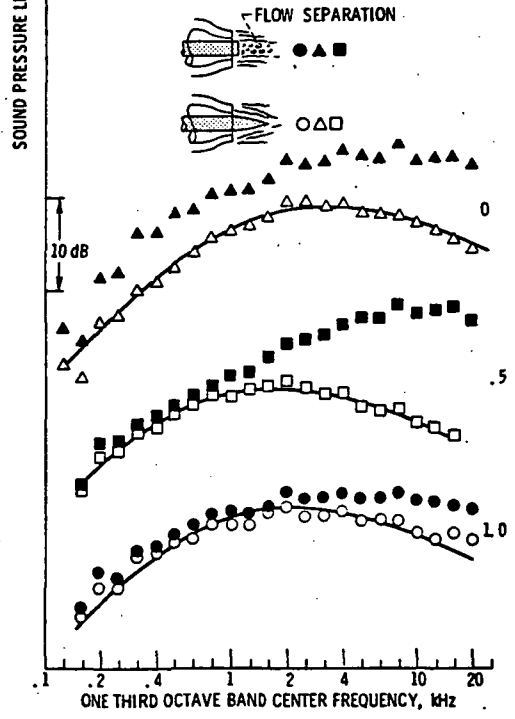
Figure 10. - Variation in peak noise frequency, relative to the core alone peak frequency.



CORE NOZZLE	CORE DIAMETER, IN.	CORE AREA, IN ²	AREA RATIO
◇ CONE PLUG	4.0	6.43	3.34
● CIRCULAR COPLANAR	3.0	7.06	3.85
○ CIRCULAR COPLANAR	4.0	12.6	3.63
□ CIRCULAR CORE, EXTENDED, $L_c/h = 8.5$	2.34	4.30	3.26



(a) COMPARISON OF PLUG CORE NOZZLE WITH VARIOUS CIRCULAR CORE NOZZLES. DATA SCALED SLIGHTLY TO PLUG NOZZLE AREA AND AREA RATIO.



(b) EFFECT OF FLOW SEPARATION OFF PLUG.

Figure 11. - Effect of a plug core nozzle on noise spectra at 90°. Plug diameter, 2.8 inch; core velocity, 985 ft/sec; environmental temperature, 77° F; free field lossless data taken on a 15 feet radius.



VELOCITY RATIO, $VR = V_F/V_C$	CORE LENGTH/ANNULUS HEIGHT L_C/h	
	8.5	56.0
1.0	□	■
.5	△	▲
0	○	●
V_E/V_F	1.0	0.5

CURVES DRAWN FROM PWL SPECTRAL SHAPE IN REF. 6

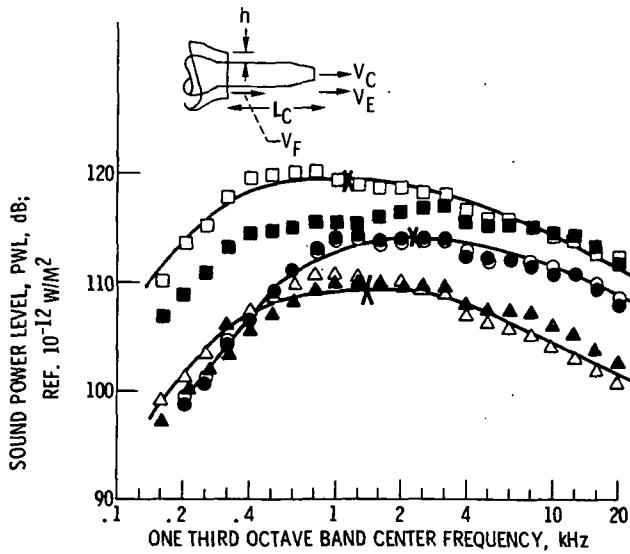


Figure 12. - Effect of a long core nozzle extension. Annulus height, h , 0.75 in.; core nozzle exit diameter, 2.34 in.; area ratio, 3.26, core jet velocity, 985 ft/sec. Environmental temperature, 77° F; free field lossless data.



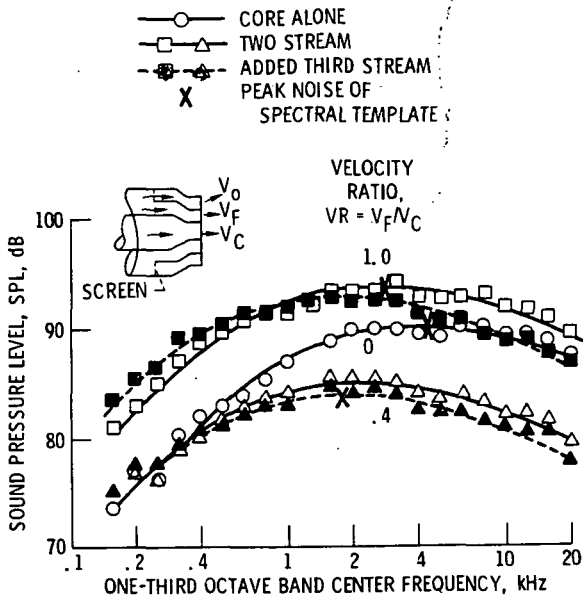
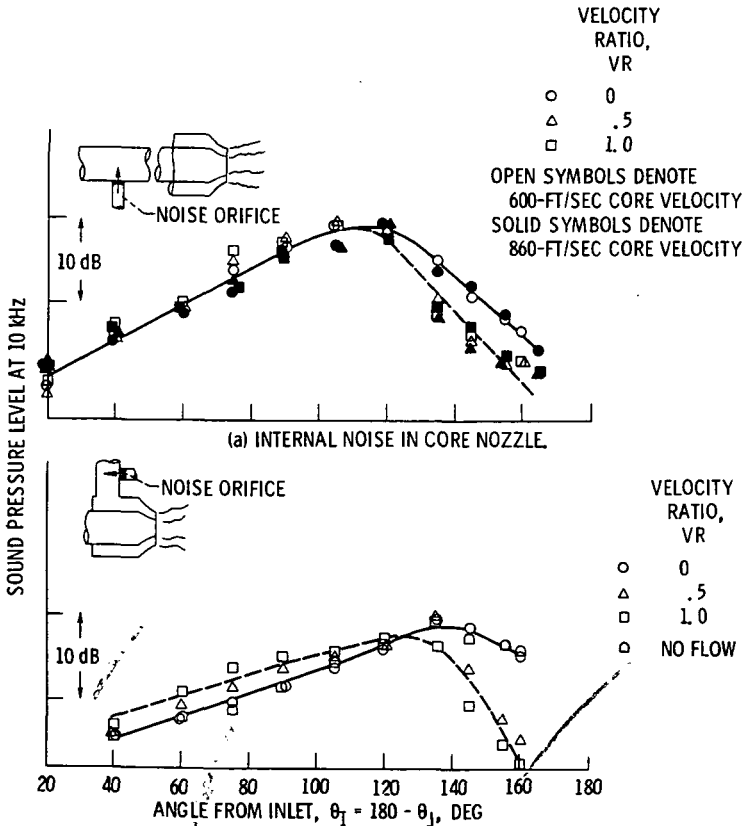


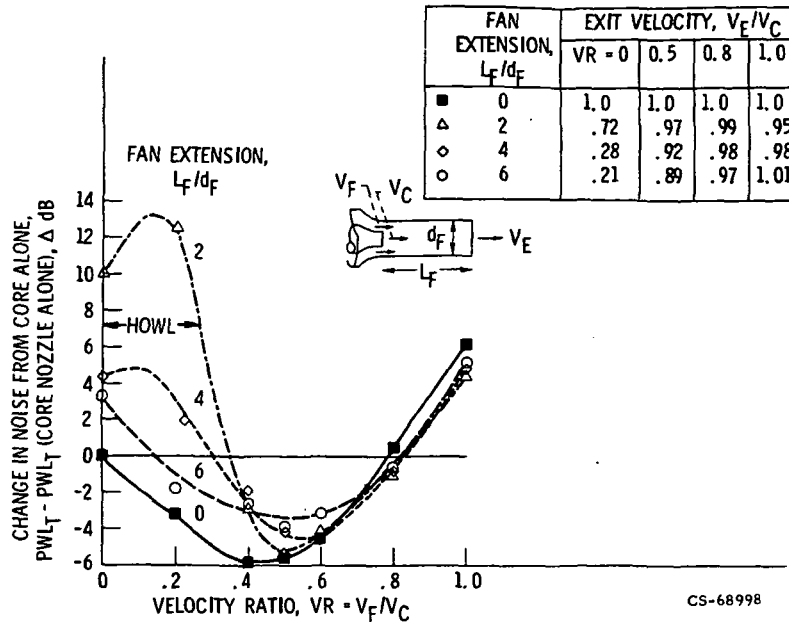
Figure 14. - Effect of a third nozzle exhaust stream. Core diameter, 3 inches; fan to core ratio, $A_F/A_C = AR$, 2.1; outer to fan area ratio, A_O/A_F , 0.78; core jet velocity, 985 ft/sec; nominal outer to fan velocity ratio, V_O/V_F , 0.75; environmental temperature, 77° F; free field lossless data on a 15-foot radius.



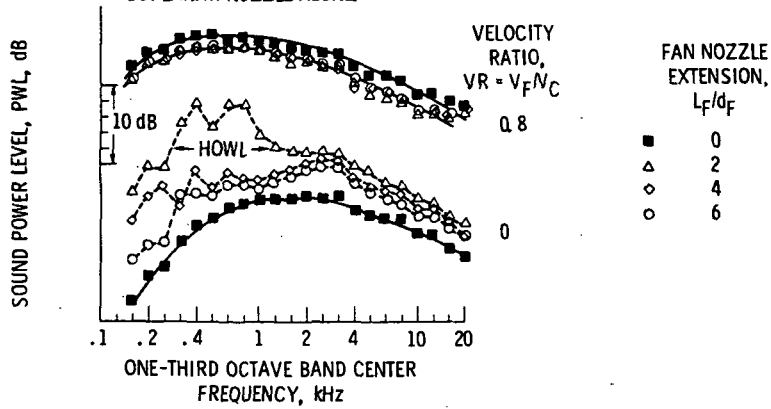
(b) INTERNAL NOISE IN FAN NOZZLE: CORE JET VELOCITY, 600 FT/SEC.

Figure 15. - Noise radiation pattern at 10 kHz of a dominant internal noise. Core diameter, 3 inches; area ratio, 2.1; noise orifice pressure ratio, 5.4





(a) CHANGE IN TOTAL POWER WITH VELOCITY RATIO; REFERENCED TO THE COPLANAR NOZZLE ALONE



(b) POWER SPECTRA AT A HIGH AND LOW VELOCITY RATIO.

Figure 13 - Effect of fan nozzle extension pipe. Core diameter, 3 inches; area ratio, 3.9; core jet velocity, 740 ft/sec; environmental temperature, 77° F; free field lossless data.